REPORT DOCUMENTATION

AD-A263 206

1. AGENCY USE ONLY (Leave blank)	2. REPORT DATE	3. REPORT TYPE AND DATES COVERED
	April 5, 1993	Reprint

4. TITLE AND SUBTITLE

The Effect of the March 1991 Storm on Accumulated Dose for Selected Satellite Orbits: CRRES Dose Models

5. FUNDING NUMBERS

PE 62101F
PR 7601
TA 22
WU 03

6. AUTHOR(S)

M.S. Gussenhoven, E.G. Mullen, Michele Sperry, K.J. Kerns, J.B. Blake*

7. PERFORMING ORGANIZATION NAME(S) AND ADDRESS(ES)

Phillips Lab/GPSP
29 Randolph Road
Hanscom AFB, MA 01731-3010

8. PERFORMING ORGANIZATION REPORT NUMBER

PL-TR-93-2079

9. SPONSORING/MONITORING AGENCY NAME(S) AND ADDRESS(ES)

10. SPONSORING/MONITORING AGENCY REPORT NUMBER

11. SUPPLEMENTARY NOTES

*The Aerospace Corporation, Los Angeles, CA 90009
Reprinted from IEEE Transactions on Nuclear Science, Vol. 39, No. 6, December 1992

12a. DISTRIBUTION/AVAILABILITY STATEMENT

Approved for public release; Distribution unlimited

12b. DISTRIBUTION CODE

13. ABSTRACT (Maximum 200 words)

Three dose models are constructed using direct measurements of dose on the CRRES satellite, in a low-inclination, geosynchronous-transfer orbit. The Average Model uses data taken over the entire 14 months of the CRRES mission from July 1990 to October 1991. The Quiet Model uses data from July 1990 to March 1991. The Active Model uses data from March 1991 to October 1991. The separation of the quiet and active periods is based on the 24 March 1991 solar particle event and subsequent solar wind shock which rearranged the inner magnetosphere radiation populations. The dose models are dose rate averages in grids of L and B/B_0. A software program (CRRESRAD), developed for the models, allows the calculation of dose behind 4 shielding thicknesses for any satellite orbit. In the active period, dose acquired in a circular, low-inclination orbit in the "slot region" is greater than in the quiet period by up to two orders of magnitude, making this region, heretofore thought to be relatively benign, comparable in radiation harshness to the peak of the inner radiation belt. The suitability of the CRRES dose models for evaluating dose in high inclination orbits is also discussed.

14. SUBJECT TERMS	15. NUMBER OF PAGES
Accumulated dose, Satellite, Dose Model, Radiation	8
	16. PRICE CODE

17. SECURITY CLASSIFICATION OF REPORT	18. SECURITY CLASSIFICATION OF THIS PAGE	19. SECURITY CLASSIFICATION OF ABSTRACT	20. LIMITATION OF ABSTRACT
UN CLASSIFIED	UNCLASSIFIED	UNCLASSIFIED	SAR

PL-TR-93-2079

IEEE TRANSACTIONS ON NUCLEAR SCIENCE, VOL. 39, NO. 6, DECEMBER 1992

The Effect of the March 1991 Storm on Accumulated Dose for Selected Satellite Orbits: CRRES Dose Models

M.S. Gussenhoven, E.G. Mullen, Michele Sperry, K.J. Kerns
Phillips Laboratory, GPSP, Hanscom AFB, MA 01731

J.B. Blake
The Aerospace Corporation, Los Angeles, CA 90009

Abstract

Three dose models are constructed using direct measurements of dose on the CRRES satellite, in a low-inclination, geosynchronous-transfer orbit. The Average Model uses data taken over the entire 14 months of the CRRES mission from July 1990 to October 1991. The Quiet Model uses data from July 1990 to March 1991. The Active Model uses data from March 1991 to October 1991. The separation of the quiet and active periods is based on the 24 March 1991 solar particle event and subsequent solar wind shock which rearranged the inner magnetosphere radiation populations. The dose models are dose rate averages in grids of L and B/B_0. A software program (CRRESRAD), developed for the models, allows the calculation of dose behind 4 shielding thicknesses for any satellite orbit. In the active period, dose acquired in a circular, low-inclination orbit in the "slot region" is greater than in the quiet period by up to two orders of magnitude, making this region, heretofore thought to be relatively benign, comparable in radiation harshness to the peak of the inner radiation belt. The suitability of the CRRES dose models for evaluating dose in high inclination orbits is also discussed.

I. Introduction

A major goal of the CRRES (Combined Release and Radiation Effects Satellite) program is to update the NASA radiation belt models [1, 2, 3] which are widely used by the space engineering community in satellite design and orbit determination. An aspect of this goal is to create models that more accurately reflect the dynamic nature of the belts. The CRRES satellite was operational from 25 July 1990 to 12 October 1991. In March 1991, a very large solar particle event combined with the near-Earth passage of a shocked solar wind provided so much energy to the inner magnetosphere that the radiation belts took on very different profiles from those in the NASA models [4]. Two new belts were formed: a second high energy proton belt with peak fluxes at an L-value of 2.25 R_E (R_E is an Earth radius) and a third electron belt with peak fluxes at an L-value of 2.15 R_E composed of electrons with energies from 1 MeV up to and exceeding 30 MeV. Electrons above ~10 MeV had not previously been measured in the inner magnetosphere [5]. These new belts filled the "slot" region between the inner (predominantly proton) belt and the outer electron belt with a very damaging particle population. For electrons, the energies are greater than those measured in either the inner or the outer belts. The new belts were still in existence some 6-plus months after their formation when CRRES ceased transmitting data due to battery failures.

The dynamic nature of the inner magnetosphere is not included in any existing model, and presents a problem for orbit planning and satellite design when cost-effective missions are imperative. A comparison of dose measurements on CRRES with NASA model predictions was previously reported [6]. The comparison showed the extreme inadequacy of NASA AE8 [7] electron dose predictions for energies greater than 5 MeV following the March event. Here we use the CRRES dose data to make statistical dose models for three periods, before and after the March storm, separately, and over the entire CRRES mission. We then use these models to calculate the dose that would be received in various satellite orbits behind four thicknesses of shielding. We show that, in selected orbits, the dose can increase by more than two orders of magnitude, and that the slot region becomes comparable to the heart of the inner belt with respect to dose accumulation behind thick shielding. Although we do not have a sufficient baseline with the CRRES data to answer every question regarding the dynamics of the near-Earth radiation environment, we can give what may be a best and a worst case dose prediction for specific orbits during solar maximum based on the CRRES measurements.

II. Instrument And Orbit

CRRES was in a low-inclination (18.2°) geosynchronous-transfer orbit, passing through the heart of the radiation belts twice every 10-hour orbit period. The satellite was equipped with the finest complement of high energy particle experiments ever flown in space. One of the instruments, the Space Radiation Dosimeter, directly measured dose acquisition as a function of time (thus, altitude and magnetic latitude). The data from this experiment are used in this report. The dosimeter returned dose data in two energy deposition ranges: 50 keV to 1 MeV, the LOLET (low linear energy transfer) range; and 1 to 10 MeV, the HILET (high linear energy transfer) range. The dose was measured behind four thicknesses of hemispherical aluminum shielding (0.57, 1.59, 3.14, 6.08 gm/cm^2) which allow penetration of electrons with energy greater than 1, 2.5, 5, and 10 MeV, respectively, and penetration of protons with energy greater than 20, 35, 52, and 75 MeV, respectively. A 1/2 inch thick tungsten base prevented

protons and electrons with energies below 120 and 200 MeV, respectively, from penetrating the detectors from underneath. The LOLET channels received energy deposition from electrons and >130 MeV protons. The HILET channels received energy deposition from protons. More complete descriptions of the dosimeter can be found in Refs 8,9.

III. Approach

Magnetospheric radiation-belt particles have been shown to be well-ordered by the McIlwain L-parameter [10] and the ratio (B/B_0) of the magnetic field intensity (B) to the field intensity of the same field line at the magnetic equator (B_0). These are commonly called L-B/B_0 coordinates. The L-parameter (simply called L) marks particle drift shells by their equatorial distance from the center of the Earth, and is measured in Earth radii (R_E). For a dipole field, L is equivalent to altitude in the magnetic equatorial plane. More complicated field models are, in effect, projected onto the dipole field to determine L. The CRRES modeling effort uses the field model that results from combining the International Geomagnetic Reference Field (IGRF) Revision 1985 internal field model [11] with the Olson-Pfitzer quiet external field model [12]. The CRRES orbit covers L-values of 1.1 to 8 R_E. B/B_0 is directly relatable to magnetic latitude. The CRRES orbit covers B/B_0 values from 1 to ~4, or magnetic latitudes from 0° to ~ ±30°. The dose maps that we create are statistical averages of data in discrete L and B/B_0 bins. The L-bin divisions are every 1/20th of an R_E; the B/B_0 divisions are variable, being equivalent to steps of 2° in magnetic latitude in a dipole field.

To create the dose models we first divided the entire CRRES dosimeter data base into two parts: that occurring before the March storm (27 July 1990 to 19 March 1991) and that after the storm (31 March 1991 to 8 October 1991). The period from 19 to 31 March was the period of the reconfiguration of the belts. It is included in an additional total data base which is used to produce the Average Model. A separate model was created from the data for each of these three time periods, and for both LOLET and HILET data. Second, we accumulated the data in L Shell- and B/B_0-bins for each CRRES orbit, by channel, and stored the total counts with the number of observations. The data from all orbits appropriate to a given model were then combined by performing a simple average over all measurements falling into each L-B/B_0 bin. Third, we corrected the data for the onboard alpha source used to update the dosimeter calibration in-flight. The correction was significant for the HILET channels and, in particular, for the first HILET channel. The alpha source was the first order limitation on the accuracy of the dose measurements. Fourth, where bin averages were suspect we set the values to zero. Bin averages were zeroed for the following reasons: a) the number of observations for the bin average was less than 450 (equivalent to 30 minutes of data collection); b) the residual after applying the alpha source correction was negative; c) the average was less than the alpha source count plus twice the statistical deviation in the alpha source count (two sigma); d) the bins were at altitudes below the low altitude cutoff of the inner belt (these points were sporadic and easily identified). Otherwise all data points were retained. Finally, the corrected dose counts were converted to dose, using pre-flight calibration results, and kept in tabular form in rads(Si)/s.

We designate the pre-event, post-event, and total data base dose models the "Quiet," "Active," and "Average" Dose Models, respectively. As we show in the next two sections, dose accumulated from the models can be quite different depending on satellite orbit.

IV. Quiet And Active Dose Models During Solar Maximum

Figures 1 and 2 are line plots taken from the Quiet and Active CRRES Dose Models, respectively. The dose is measured behind dome 2, which has a thickness of 232.5 mils Al. The figures show the dose in rad(Si)/s as a function of L and averaged for the three B/B_0 values nearest the magnetic equator (±6° around the magnetic equator). They are shown only out to L-values of 6.5, because they become discontinuous and near background beyond this value. The HILET (LOLET) dose is shown with large (small) dashed lines. The total dose is shown with a solid line. HILET dose dominates for $L < 2\ R_E$, and LOLET dose for $L > 3\ R_E$.

In the Quiet Model (Figure 1) there is a clear slot region between 2 and 3 R_E separating the inner and outer radiation belts. This region is relatively benign, having a dose rate almost 500 times less than the peak of the inner belt and an order of magnitude less than the peak of the outer belt. A major difference between the Quiet Model and the Active Model (Figure 2) is that the slot region is filled with a second HILET belt and a third LOLET belt. The peak of the new LOLET belt (2.15 R_E) is somewhat nearer the Earth than the peak of the new HILET belt (2.25 R_E). The peak intensity of the new LOLET belt is greater than both the inner and the outer LOLET belt peak intensity, while the intensity of the new HILET peak is only somewhat (30%) less than that of the inner belt. Thus, the slot region is filled with a new radiation belt that is comparable in intensity to that of the inner belt, which was previously assumed to be the region of greatest radiation hazard in the magnetosphere.

Other points of comparison are: The inner belt is unchanged in the two models. The LOLET outer belt peaks somewhat closer to the Earth and is about an order of magnitude more intense in the Active Model compared to the Quiet Model. At high L values ($>3\ R_E$) the HILET dose rate in the Active Model is greater, by about an order of magnitude, than that in the Quiet Model. This is due to the greater number of solar proton events during the active period and the ability of these protons to penetrate deeply into the magnetosphere.

Figure 3 shows the Active Model dose rate as a function of L for B/B_0 = 1.69-1.88 [±(20° - 22°)] Magnetic Latitude). Here we see that the total dose in the inner belt and the slot

region belt is diminished by about a factor of 5, but that the outer LOLET belt remains at the same intensity. The dose in the new belt is almost entirely LOLET dose, the HILET dose being severely diminished at this distance from the magnetic equator. These profiles indicate that the LOLET dose particles (primarily electrons) are far more isotropic than the HILET dose particles (primarily protons), and that the protons in the new belt are much more strongly confined to the magnetic equator (have deeper loss cones) than those in the inner belt. The particles in the new belt are trapped with long lifetimes and were measured from 24 March 1990 until CRRES stopped transmitting data, 12 October 1991.

One can use profiles such as those in Figures 1-3 to estimate directly what dose will be encountered by satellites in low inclination orbits. By using the entire dose models for each shielding thickness, the dose can be more accurately calculated by using orbit elements to determine dwell times over a satellite lifetime in each L and B/B_0 bin and accumulating the dose using the appropriate dose rate from the models. We have created a software program, called CRRESRAD, which can be run on a personal computer to do this [13]. This method of estimating dose for a satellite mission differs from the way dose is estimated using the NASA radiation models. The NASA radiation models give integral electron and proton omnidirectional fluxes above set thresholds for points on an L-B/B_0 grid. To determine dose from these particles behind a shielding of given shape and thickness, a transport code must be used. These codes are fairly straight-forward for protons, but quite complex for electrons. Creating dose models from in-space measurements eliminates the need for such codes. However, the dose model is, in this case, for one shielding shape (hemispherical dome) and for four shielding thicknesses, and is, therefore, much less flexible than a particle flux model. The main advantage of using a dose model is that it gives accurate total dose, including effects from Bremsstrahlung, without having to use transport codes. In the two next sections, we demonstrate how the program can compute dose using the CRRES model a) to show the difference between the quiet and the active periods for low inclination orbits at various altitudes where CRRES data exists, and b) to get somewhat limited dose information for high inclination orbits.

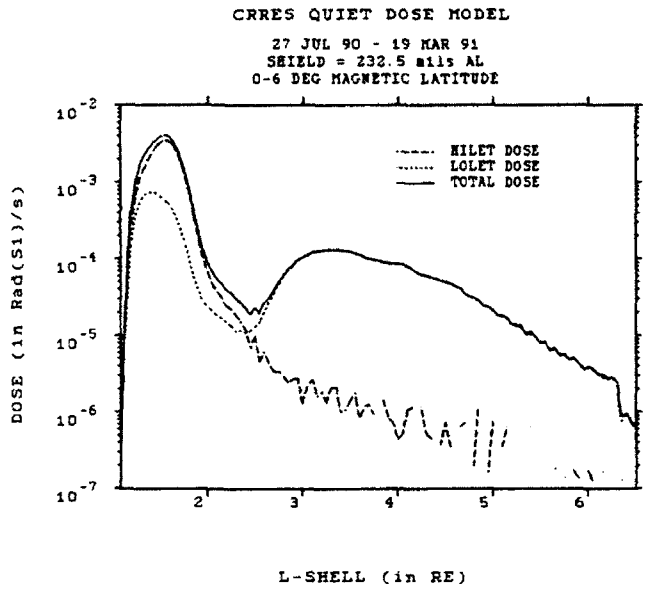

Figure 1. Dose rate, in Rad(Si)/s, as a function of L, in R_E, for the CRRES Quiet Dose Model. The dose is accumulated within 6^0 of the magnetic equator. HILET (LOLET) dose is plotted with a thick (thin) dashed line; total dose is plotted with a thick, solid line.

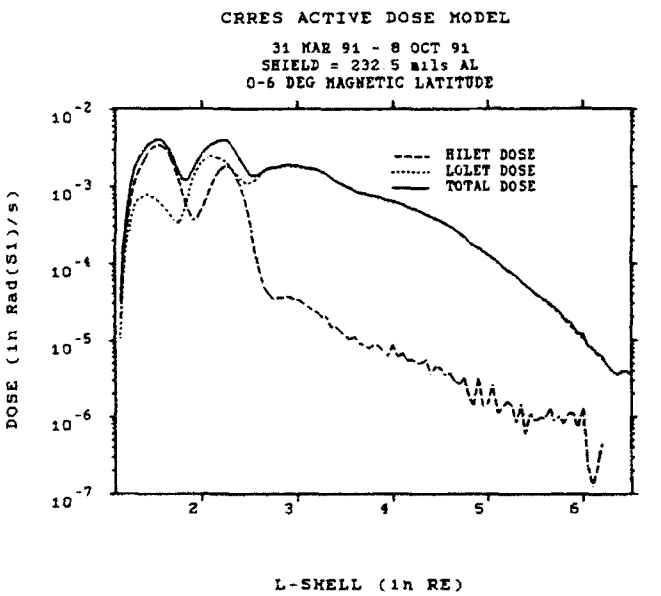

Figure 2. Same as Figure 1, but for the CRRES Active Dose Model.

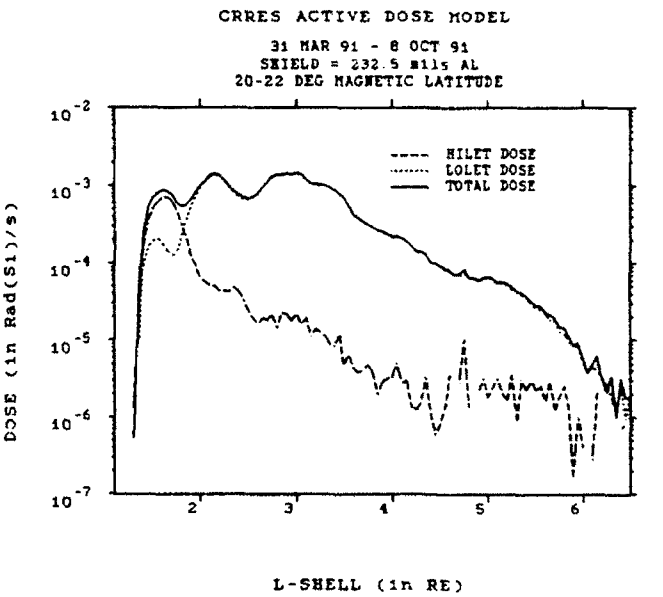

Figure 3. Same as Figure 2, but for dose accumulated between $20\text{-}22^0$ magnetic latitude.

V. Results for Low Inclination Orbits

To give some indication of worst case scenarios for periods before and after the March event, we have run several circular, 0°-inclination orbits through the models represented by Figures 1 and 2 at altitudes either where maximum dose would be expected or where some satellites operate. The results are given for 5 altitudes and 4 shielding thicknesses in Table 1. The altitudes are given as distances from the center of the Earth in Earth radii. The orbits chosen are a) a circular orbit at 1.55 R_E passing through the heart of the inner belt, b) two circular orbits (one at 2.2 R_E and one at 2.5 R_E) that pass through the slot region, c) a circular orbit at 3.5 R_E that passes through the heart of the outer belt, and d) a geosynchronous orbit at 6.6 R_E. We have also included the measured dose (projected to dose per year) on CRRES, in a geosynchronous transfer orbit at 18° inclination, for the two periods. As would be expected, the measured CRRES dose and that found by running the CRRES orbits through the dose models (not shown) agree within a few percent.

Several conclusions may be drawn from the table:

A) The inner belt at the peak dose intensity altitude of 1.55 R_E is constant before and after the event.

B) The dose in the slot region near 2.20 R_E increases by a factor of 30 to 100 depending on shielding thickness, and becomes greater than the dose in the heart of the inner belt behind shielding thicknesses greater than 1/2 inch Al (Domes 3 and 4).

C) The dose at the outer edge of the newly formed belt, at 2.5 R_E, is still approximately 50 times higher than the pre-event level.

D) The dose at the peak of the outer belt (3.5 R_E) reflects the dynamic behavior of electrons and changes by about a factor of 10 in an average sense before and after the event.

E) There is a small dose increase at geosynchronous altitude for thinner shieldings in the active period. However, the variations are more a function of the number of large particle events (both electron and proton) than average dose levels.

F) For the CRRES orbit, a geosynchronous transfer orbit, the total orbit dose changed by about a factor of 3 for all shielding levels between quiet and active periods.

We note that prior to the March event the slot region between 2.2 and 2.5 R_E is almost as benign a radiation region as the region at geosynchronous altitude. For this reason low altitude satellite orbits are sometimes designed with apogee in or near the slot region. Figures 4 and 5 show the dose depth curves for HILET and LOLET dose, respectively, before and after the March storm, for a circular, 0°-inclination orbit at 2.20 R_E. Also added to these plots are the dose-depth curves for the most severe environment, a circular, 0°-inclination orbit at the heart of the inner radiation belt, at 1.55 R_E.

TABLE 1.
COMPARISON OF DOSE (kRads/Year)
BEFORE (AFTER) MARCH, 1991 STORM

Circular, 0° Inclination Orbits and CRRES Orbit

SHIELDING THICKNESS gm/cm²	0.57	1.59	3.14	6.08
INNER BELT Circular, r=1.55 R_E	474.8 (485.1)	103.7 (104.8)	54.7 (56.2)	29.2 (30.9)
SLOT REGION A. Circular, r=2.20 R_E	3.5 (109.0)	1.1 (85.8)	0.8 (78.4)	0.3 (33.9)
SLOT REGION B. Circular, r=2.50 R_E	2.0 (119.2)	0.6 (43.8)	0.3 (20.3)	.14 (6.2)
OUTER BELT Circular, r=3.50 R_E	205.7 (1169.9)	3.6 (28.9)	0.3 (2.16)	0.2 (1.0)
GEOSYNCHRONOUS Circular, r=6.60 R_E	2.3 (9.5)	0.02 (.11)	0.01(0.03)	0.01 (0.01)
CRRES* Geosynchronous Transfer	60 (210)	3.3 (12)	1.8 (5.2)	0.99 (2.6)

*Measured orbit by orbit, not from CRRES model

For HILET (proton) dose the two orbits differ in dose by about two orders of magnitude before the storm and by much less than one order of magnitude after the storm. On the other hand, LOLET dose (electron and >130 MeV protons) for the orbit in the slot region after the storm exceeds that for the orbit in the inner belt.

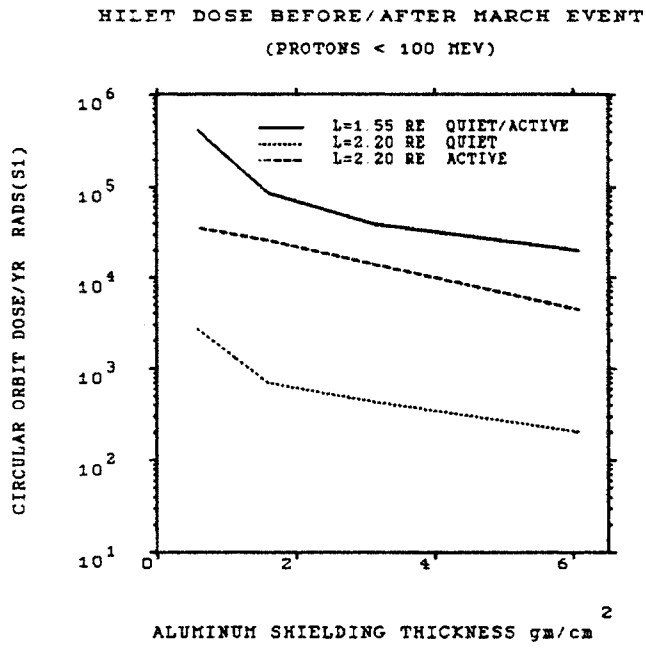

Figure 4. HILET dose rate (in Rads(Si)/year) as a function of shielding thickness for two 0° inclination, circular satellite orbits using the Quiet (dotted line) and Active (dashed line) CRRES Dose Models. The orbit with altitude L=1.55 R_E (thick line) is through the heart of the inner radiation belt and receives the same dose in both models. The orbit with altitude 2.2 R_E (dashed lines) is in the slot region.

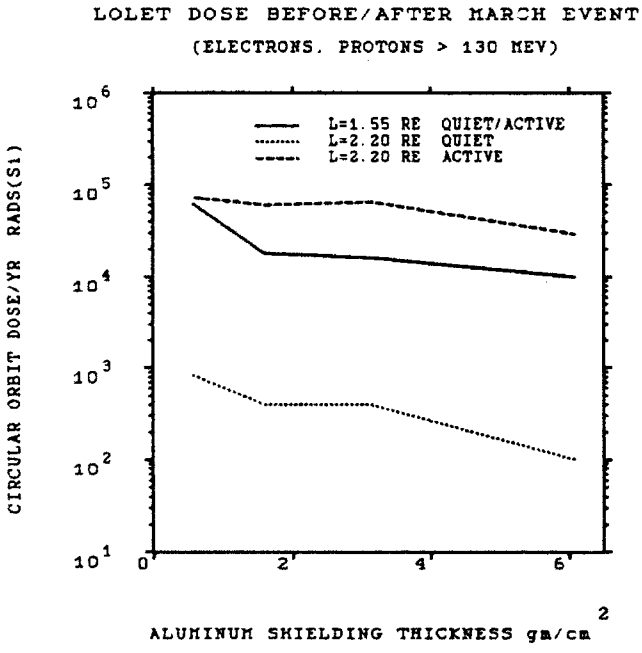

Figure 5. Same as Figure 4, but for LOLET dose rate.

VI. The CRRES Dose Models and High Inclination Orbits

The CRRES orbit limits the region of space sampled to $\pm 30^0$ in magnetic latitude and to about 6.5 R_E from the center of the Earth. This limits, in turn, the region of the CRRES dose models. There are a number of ways in which the CRRES empirical dose models can be extrapolated to higher magnetic latitudes, or interpolated between CRRES positions and those of a different satellite on which dose is measured, eg., DMSP, in order to increase the model applicability. We intend to pursue these means of extending the models. However, the CRRES model can be used as it is for high inclination orbits if the dose of interest is that produced primarily by protons, or if it is accumulated behind thick shielding (>200 mils Al), because almost the entire population of particles producing these doses is contained within the CRRES sampling region. This is because the fall-off in dose rate with B/B_0 is fast for L values less than 2.5 R_E. Thus, little error will be made in dose acquisition for those high inclination satellite orbits whose apogees lie below L-values of 2.5 R_E. Above L = 2.5 R_E, however, in the region of the outer zone electrons, the dose is not so tightly confined to the magnetic equatorial plane, and must be extrapolated for higher B/B_0 values. To show this we compare dose predicted from the CRRES model for the DMSP satellites to measurements of dose made on DMSP by a dosimeter similar to that flown on CRRES. The DMSP measurements have been previously reported [9, 14, 15]. We note that additional belts in the slot region were also measured by DMSP in conjunction with the solar particle event and large magnetic storm that occurred in early February 1986 [14].

The DMSP satellite orbits are near-circular (840 km altitude), polar (98° inclination), sun-synchronous orbits. The DMSP/F7 satellite, carrying a dosimeter, returned data from December 1983 to October 1987. This period encompassed the last solar minimum occurring in September 1986. Average daily dose rates for each of the dosimeter channels were calculated in monthly intervals [15]. For HILET (protons), the minimum average daily dose occurred at the beginning of the mission, that is, closest to solar maximum, and rose steadily throughout the mission. For LOLET (electrons and >100 MeV protons) the average daily dose behind the thinnest shielding was highly variable, but behind the other three domes increased more or less steadily over the mission.

Table 2 gives the comparison between the dose predicted for DMSP from the CRRES models (the dose does not change appreciably between quiet and active models) and the monthly minimum and maximum dose rates measured on DMSP. All dose values are projected to a yearly dose. The dose, in each case, is divided into HILET and LOLET ranges. The comparison of HILET dose to the minimum dose measured by DMSP is excellent (within 8%). The minimum dose values measured on DMSP are those closest to solar maximum, and, thus, more appropriate for comparison to CRRES data. The HILET maximum values measured on DMSP were taken thir-

TABLE 2.
COMPARISON OF CRRES MODEL DOSE
AND MEASURED DOSE
FOR THE DMSP ORBIT in Rads(Si)/Year

SHIELDING THICKNESS in gm/cm^2	CRRES MODEL DOSE		DMSP MONTHLY AVERAGED DOSE MINIMUM (MAXIMUM)	
	HILET	LOLET	HILET	LOLET
0.57	359	207	376 (504)	223 (2300)
1.59	255	129	266 (358)	135 (142)
3.14	223	124	204 (266)	95 (106)
6.08	152	96	157 (266)	- -

teen months after solar minimum. They are well within a factor of two of the CRRES predictions, which is the rule-of-thumb difference for protons at solar minimum and solar maximum. The LOLET comparisons between the CRRES model values and the measured values are reasonably good (< 25%) for the middle two shielding levels. (Lack of good thermal control of the dosimeter on DMSP voided the LOLET measurements behind the thickest shielding for much of the mission). The comparison is also good for the thinnest shielding when compared to the minimum value measured on DMSP. It is an order of magnitude less than the maximum value. In the CRRES model runs, 54% of the DMSP orbit is outside of the region of the model. Clearly, electrons at high magnetic latitudes make a significant contribution to dose behind thin shielding for high inclination orbits and these are not yet included in our dose models. For protons, and for thick shields, the CRRES dose models are also applicable to high inclination orbits.

VII. DISCUSSION AND CONCLUSIONS

The CRRES dose data have been used to model two very different conditions in the radiation belts: a quiet condition with an inner belt and an outer electron belt; and an active condition in which a third belt, composed of protons and extremely energetic electrons, fills the slot region. An Average Dose Model has also been constructed using all the CRRES data. Dynamics are very important in considering how and when to use the models. A peculiarity of the models is that the high altitude HILET model has both zero and non-zero bins which result from the infrequent occurrence of solar proton events that last for several consecutive orbits. Indicators of solar and magnetospheric conditions averaged over the time periods of the models can help in evaluating the applicability of the models. These are listed in Table 3 for the Quiet and Active model periods. The averages were constructed from preexisting daily averages. The average sunspot number [16] is essentially the same for the two periods, indicating that all the data were taken at the same position in the solar cycle. The high energy solar proton and electron fluxes [16] measured at geosynchronous altitude by the GOES satellite are ~20 and 6 times greater, respectively, for the active period than for the quiet period, and provide the biggest difference we see in the Table 3 values. These particles are thus a possible strong driver of radiation belt dynamics. The polar rain (low energy electron precipitation over the polar caps and taken here from the polar cap with the larger flux value [17]) is about 50% greater during the active period than the quiet period indicating a decrease in the difference between the solar wind speed and the Alfven speed [$B(4\pi n)^{-1/2}$] for active times. This may indicate the importance of Alfven waves (plasma waves that propagate at the Alfven speed and are the result of a restoring force provided by the magnetic field) on the surface of the magnetosphere for activating the belts. Of the three magnetospheric activity indices, K_p [18], D_{st} [19] and the position of the auroral boundary at local midnight [20], only D_{st}, measuring the inner magnetospheric ring current, shows a major difference (about a factor of 2.5). The ring current, is a regular feature of magnetic storms and probably the best indicator of a long interval of storm dynamics [21]. Auroral or substorm activity, as indicated by K_p, and the size of the auroral oval (midnight boundary) is the same for both periods, on average.

All of the new CRRESRAD models apply to solar maximum conditions. Differences in orbital dose between quiet and active conditions can exceed two orders of magnitude. Because of this, radiation belt dynamics must be considered in mission planning, particularly for satellites that spend much of

TABLE 3.
INDICATORS OF SOLAR OR MAGNETOSPHERIC ACTIVITY
Average Values

	"QUIET" PERIOD 27 Jul 1990-19 Mar 1991	"ACTIVE" PERIOD 31 Mar 1991-8 Oct 1991
Sunspot Number	223	219
GOES >10 MeV Proton Flux	1.2 10^5 $(cm^2\ day\ sr)^{-1}$	20.2 10^5 $(cm^2\ day\ sr)^{-1}$
GOES >2 MeV Electron Flux	1.1 10^7 $(cm^2\ day\ sr)^{-1}$	6.7 10^7 $(cm^2\ day\ sr)^{-1}$
Polar Rain Intensity	6.7 10^6 $(cm^2\ s\ sr)^{-1}$	9.1 10^6 $(cm^2\ s\ sr)^{-1}$
K_p	2.2	2.2
D_{st}	-12.2	-31.5
Auroral Boundary	63.3° Magnetic Latitude	61.3° Magnetic Latitude

their time in the slot region. Software, called CRRESRAD, has been developed to estimate dose behind the four thicknesses of shielding used on the CRRES dosimeter for any closed satellite orbit the user specifies. It quickly estimates mission dose using the CRRES Quiet, Active and Average dose models. Even though the CRRES models only extend to 30° around the magnetic equator, the models will give reasonable dose predictions for high inclination orbits if the shielding is greater than about 1/4 inch Al, as shown in Table 2.

VIII. ACKNOWLEDGEMENTS

To produce a use-friendly software package for the transition of space environment data and to provide analysis results to the spacecraft design and operations community, the efforts of many people are necessary. The CRRESRAD software utility has intermittently drawn on the expertise of many of the CRRES team over a decade in order to reach fruition. To all the CRRES participants who made CRRES a successful mission, we say "Thanks for a job well done." Special appreciation goes to Fred Hanser and Bronislaw Dichter of Panametrics Inc. for the design, development, test and calibration of the Space Radiation Dosimeter which collected the data used in CRRESRAD. We wish to thank Karl Pfitzer of McDonnell Douglas for providing and adapting the magnetic field model used for binning and retrieving the data in CRRESRAD. We thank Kris Bhavnani, Bill McNeil, and Jim Bass of RADEX Inc. who did an excellent job of providing the ephemeris routines needed to store and retrieve the data. And finally a special thanks to the data reduction and software development team at Boston College (Ernie Holeman, Dan Madden, Dennis Delorey and Paul Pruneau) who transformed the raw data into geophysical quantities and developed many of the graphics tools used in the study.

IX. REFERENCES

[1] Vette, J.I., M.J. Teague, D.M. Sawyer, and K.W. Chan, "Modelling the Earth's Radiation Belts," in Solar-Terrestrial Prediction Proceedings, Vol. 2, edited by R.F. Donnelly, U.S. Department of Commerce, NOAA, Boulder, 1979.

[2] Vette, J.I., King W. Chan, and M.J. Teague, "Problems in Modelling the Earth's Trapped Radiation Environment," AFGL-TR-78-0130, ADA059273, 1978.

[3] Spjeldvik, W.N. and P.L. Rothwell, "The Radiation Belts," Chapter 5 in Handbook of Geophysics and the Space Environment, edited by Adolph S. Jursa, Air Force Geophysics Laboratory, Hanscom AFB, MA, ADA167000, 1985.

[4] Mullen, E.G., M.S. Gussenhoven, K. Ray, and M. Violet, "A double-peaked inner radiation belt: Cause and Effect as seen on CRRES," IEEE Trans. Nucl. Sci., 38, 1713, 1991.

[5] Blake J.B., M.S. Gussenhoven, E.G. Mullen, and R.W. Filius, "Identification of an unexpected electron space radiation hazard," submitted to this conference, 1992.

[6] Gussenhoven, M.S., E.G. Mullen, D.H. Brautigam, E. Holeman, C. Jordan, F. Hanser, and B. Dichter, "Preliminary comparison of dose measurements on CRRES to NASA Model predictions," IEEE Trans. Nucl. Sci., 38, 1655, 1991.

[7] Vette, J.I., "The AE-8 Trapped Electron Model Environment," NSSDC 91-24, NASA GSFC, Greenbelt, MD, 1991.

[8] Morel, P.R., F. Hanser, B. Sellers, H. Hunerwadel, R. Cohen, B.D. Kane and B.K, Dichter, "Fabricate, Calibrate and Test a Dosimeter for Integration into the CRRES Satellite," GL-TR-89-0152, Geophysics Laboratory, Hanscom AFB, MA, 1989.

[9] Gussenhoven, M.S., E.G. Mullen, R.C. Filz, D.H. Brautigam, and F.A. Hanser, "New low-altitude dose measurements," IEEE Trans. Nucl. Sci., 34, 676, 1987.

[10] McIlwain, C.E., "Coordinates for mapping the distribution of magnetically trapped particles," J. Geophys. Res., 66, 3681, 1961.

[11] IAGA Division I, Working Group 1, "International Geomagnetic Reference Field Revision 1985," Eos, Trans., Am. Geophys. U., 67, No. 24, 1986.

[12] Olson, W.P. and K.A. Pfitzer, "A quantitative model of the magnetospheric magnetic field," J. Geophys. Res., 79, 3739, 1974.

[13] Kerns, K.J. and M.S. Gussenhoven, "CRRESRAD Documentation," PL-TR-92-2201, Phillips Laboratory, Hanscom AFB, MA, 1992.

[14] M.S. Gussenhoven, E.G. Mullen and E. Holeman, "Radiation belt dynamics during solar minimum," IEEE Trans. Nucl. Sci., 36, 2008, 1989.

[15] Gussenhoven, M.S., E.G. Mullen, D.H. Brautigam, and E. Holeman, "Dose variation during solar minimum," IEEE Trans. Nucl. Sci., 38, 1671, 1991.

[16] Preliminary Report and Forecast of Solar Geophysical Data, U.S. Dept. Commerce, NOAA, Boulder, CO, SESC PRF 776-841, 1990-1991.

[17] Gussenhoven, M.S., and D. Madden, "Monitoring the polar rain over a solar cycle: A polar rain index," J. Geophys. Res., 95, 10399, 1990.

[18] IUGG: Association of Geomagnetism and Aeronomy (International Service of Geomagnetic Indices) Institut fur Geophysik, Postfach 2341, D-W-3400, Gottingen.

[19] World Data Center-C2 for Geomagnetism, Kyoto U., Kyoto.

[20] Madden, D. and M.S. Gussenhoven, "Auroral Boundary Index from 1983 to 1990," GL-TR-90-0358, Geophysics Laboratory, Hanscom AFB, MA, 1990.

[21] Rostoker, G., "Geomagnetic indices," Rev. Geophys. and Space Phys., 10, 935, 1972.